

**Titre:** Evidence of second order transition induced by the porosity in the  
Title: thermal conductivity of sintered metals

**Auteurs:** Aïmen E. Gheribi, Jean-Laurent Gardarein, Fabrice Rigollet, & Patrice  
Authors: Chartrand

**Date:** 2014

**Type:** Article de revue / Article

**Référence:** Gheribi, A. E., Gardarein, J.-L., Rigollet, F., & Chartrand, P. (2014). Evidence of  
Citation: second order transition induced by the porosity in the thermal conductivity of  
sintered metals. APL Materials, 2(7), 076105 (6 pages).  
<https://doi.org/10.1063/1.4886221>

## Document en libre accès dans PolyPublie

Open Access document in PolyPublie

**URL de PolyPublie:**  
PolyPublie URL: <https://publications.polymtl.ca/4889/>

**Version:** Version officielle de l'éditeur / Published version  
Révisé par les pairs / Refereed

**Conditions d'utilisation:**  
Terms of Use: Creative Commons Attribution 4.0 International (CC BY)

## Document publié chez l'éditeur officiel

Document issued by the official publisher

**Titre de la revue:**  
Journal Title: APL Materials (vol. 2, no. 7)

**Maison d'édition:**  
Publisher: AIP Publishing

**URL officiel:**  
Official URL: <https://doi.org/10.1063/1.4886221>

**Mention légale:**  
Legal notice:

# Evidence of second order transition induced by the porosity in the thermal conductivity of sintered metals

Cite as: APL Mater. 2, 076105 (2014); <https://doi.org/10.1063/1.4886221>

Submitted: 24 February 2014 . Accepted: 20 June 2014 . Published Online: 14 July 2014

Aïmen E. Gheribi, Jean-Laurent Gardarein, Fabrice Rigollet, and Patrice Chartrand



View Online



Export Citation



CrossMark

## ARTICLES YOU MAY BE INTERESTED IN

Experimental study of the thermal conductivity of sintered tungsten: Evidence of a critical behaviour with porosity

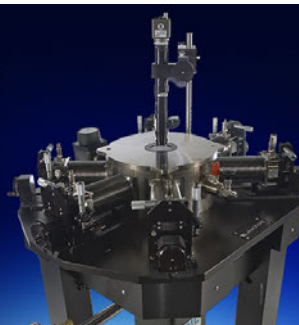
Applied Physics Letters **107**, 094102 (2015); <https://doi.org/10.1063/1.4929717>

Thermal transport properties of multiphase sintered metals microstructures. The copper-tungsten system: Experiments and modeling

Journal of Applied Physics **119**, 145104 (2016); <https://doi.org/10.1063/1.4945764>

Percolating porosity in ultrafine grained copper processed by High Pressure Torsion

Journal of Applied Physics **114**, 183509 (2013); <https://doi.org/10.1063/1.4829705>



**Cryogenic probe stations**  
for accurate, repeatable  
material measurements

LEARN MORE



## Evidence of second order transition induced by the porosity in the thermal conductivity of sintered metals

Aïmen E. Gheribi,<sup>1,a</sup> Jean-Laurent Gardarein,<sup>2</sup> Fabrice Rigollet,<sup>2</sup> and Patrice Chartrand<sup>1</sup>

<sup>1</sup>CRCT-Center for Research in Computational Thermochemistry, Department of Chemical Engineering, École Polytechnique, Box 6079, Station Downtown, Montréal, Québec H3C 3A7, Canada

<sup>2</sup>Aix-Marseille Universit, CNRS, IUSTI UMR 7343, 13013 Marseille, France

(Received 24 February 2014; accepted 20 June 2014; published online 14 July 2014)

In this paper, using both experimental data and theoretical modelling, we investigate the degradation of the thermal conductivity of sintered metals due simultaneously to the grain boundary thermal resistance and the porosity. We show that the porosity dependence of the thermal conductivity of sintered material from spherical particle powder, exhibits a critical behaviour associated with a second order phase transition. An analytical model with a single parameter is proposed to describe the critical behaviour of the thermal conductivity of sintered metals versus porosity. © 2014 Author(s). All article content, except where otherwise noted, is licensed under a Creative Commons Attribution 3.0 Unported License. [<http://dx.doi.org/10.1063/1.4886221>]

Reliable data on thermal conductivity are required for designing new alloys and modelling heat treatment processes. Thermal conductivity controls the temperature gradients occurring in materials. These temperature gradients lead to internal stress. Consequently, for transformations depending on cooling rate and temperature, the thermal conductivity is directly related to the grain size and to the residual tensile strength. The thermal conductivity is therefore an essential property for predicting the temperature dependence of the microstructure and for understanding heat treatment and solidification. Generally, the thermal conductivity of a polycrystalline material is considerably lower than its corresponding bulk crystal. This difference is mainly due to thermal resistance at the grain boundaries and to the porosity of the material. In addition, thermal conductivity of sintered materials is strongly influenced by how the materials are prepared. They are known to have different physical properties than metals produced using more conventional techniques. The predominant microstructural feature of sintered materials is their porosity. The compacting pressure used during material preparation is the principal factor defining the intrinsic porosity of sintered materials; their porosity can be as high as 60%. In recent years, there has been a growing interest in porous sintered metals in many technical areas, including heat exchangers, heat pipes, storage reservoirs for liquids, in the automotive industry and aerospace. Because of their desirable mechanical and physical properties, such as high strength, corrosion resistance, low capillarity radius, rigidity, and shock resistance, sintered metals are often the best choice. Nevertheless, their thermal conductivity remains misunderstood, especially regarding the porosity factor.

We searched the literature for recent experiments measuring the porosity dependence of the thermal conductivity of sintered metals. We found data in particular for copper,<sup>1,7,8</sup> stainless steel,<sup>2</sup> and silver.<sup>3</sup> These studies all showed that, beyond a certain porosity percentage, thermal conductivity starts to decrease drastically (with the increasing porosity). This behaviour was not well interpreted or explained by the authors. However, some analytical relations, which are expected to be suitable for describing the porosity dependence of good conducting porous materials,<sup>4</sup> were used to correlate thermal conductivity and porosity data. Nevertheless, as pointed out by Lima *et al.*,<sup>2</sup> such models cannot satisfactorily the critical behaviour, as they can provide only valuable information on the

<sup>a</sup> Author to whom correspondence should be addressed. Electronic mail: [aimen.gheribi@polymtl.ca](mailto:aimen.gheribi@polymtl.ca)

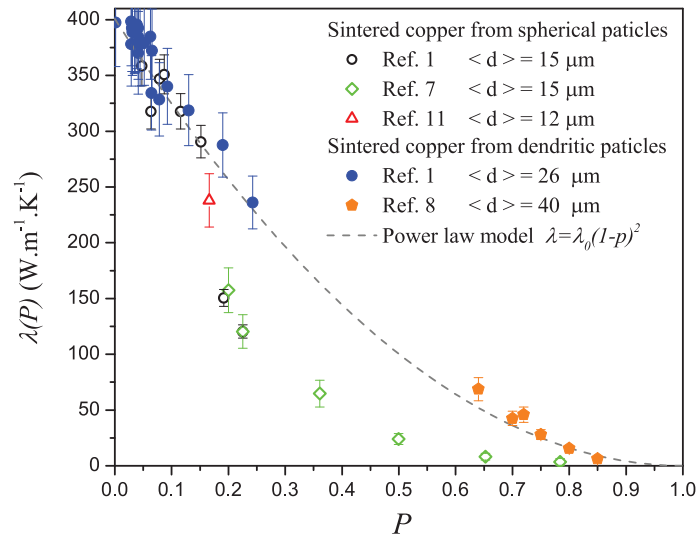


FIG. 1. Experimental available data of thermal conductivity for two types of sintered copper in comparison with the power law model (dashed line). The first type of sintered copper is obtained from spherical particles powder (open symbol) and the second type from dendritic particles powder (filled symbol).

pores sizes and distribution. The aim of this paper is to provide a possible physical interpretation of the drastic decrease of the thermal conductivity,  $\lambda$ , of sintered metals as a function of their porosity,  $P$ .

The recent experiments of Vicent *et al.*<sup>1</sup> show a very marked change of thermal conductivity of copper sintered from spherical particles above  $\approx 16\%$ . In order to confirm or disconfirm this observation, we have first measured the thermal conductivity of a sample of sintered spherical particles with a porosity of  $P = 16.6\%$ , with a laser flash method. The Cu powder was supplied by Ecka Granules Ltd at Fürth, Germany. The Cu powder has spherical particles with sizes  $< 45 \mu\text{m}$  and an average grain size of  $< 12 \mu\text{m}$ . For more details on sample preparation and microstructure, see the supplier's website.<sup>9,10</sup> The experimental procedure for the determination of thermal diffusivity of this sample is given as the supplementary material for this work.<sup>11</sup>

Fig. 1 shows the  $\lambda(P)$  curve of sintered copper obtained, respectively, from spherical and dendritic particles in comparison with the power law model:<sup>12,13</sup>  $\lambda = \lambda_0(1 - P)^n$ .  $\lambda_0$  is the thermal conductivity at zero porosity and is equal to  $401 \text{ W m}^{-1} \text{ K}^{-1}$ <sup>14</sup> for polycrystalline copper. The power law model predicted accurately the  $\lambda(P)$  curve of sintered dendritic copper in the entire range of porosity, from only the knowledge of  $\lambda_0$ . In contrast, the thermal conductivity of sintered spherical copper deviates considerably at a porosity level of about 15%, with an abrupt decrease of  $130 \text{ W m}^{-1} \text{ K}^{-1}$ . This abrupt decrease is represented in Fig. 2 through the normalized derivative of  $\lambda(P)$ :  $\chi = \lambda_0^{-1}(d\lambda/dP)$ . The form of  $\chi(P)$  is similar to the typical form of second order thermodynamic or magnetic phase transition induced by temperature (e.g., magnetic heat capacity and susceptibility or heat capacity change near order-disorder transition). A second order phase transition corresponds to spontaneously broken symmetry associated with an appropriate order parameter. In the case of magnetic phase transition, the broken symmetry is the spin rotation symmetry, and for an order-disorder transition, the broken symmetry is the crystal periodicity. In the present case, the second order phase transition is induced by the porosity. The broken symmetry is associated with the pores' environment within the microstructure. Below the critical porosity (denoted by  $P_c$ ), each pore is surrounded by grains. Above the critical porosity, pores start to be inter-connected and their density increases continuously. Above a certain porosity level the probability that a grain is surrounded by gas is non-negligible and the thermal conductivity should then decrease rapidly to zero. For a dendritic microstructure, the pores are already interconnected even at very low porosity levels ( $P_c \sim 0$ ). For an effective property for which  $P_c \sim 0$ , Kováčik and Šimančík<sup>15</sup> have shown, on the basis of the percolation theory,<sup>16</sup> that the porosity dependence of the considered property obeys the power law model. On this basis, one can assume that both the sintered copper obtained

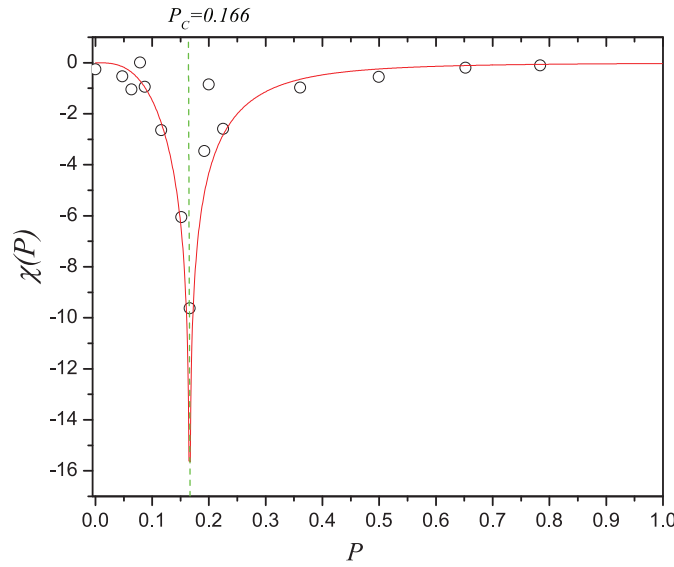


FIG. 2. Critical behaviour of the sintered spherical copper as a function of porosity. The critical porosity  $P_c = 0.166$  is indicated by a dashed line and corresponds to the position of the peak of  $\lambda_0^{-1}(d\lambda/dp)$ .

from dendritic and spherical particle powders show a critical behaviour. The critical porosities are, respectively, 0 and 0.166, and the second order phase transition, induced by the porosity, corresponds to a closed (pores are separated) to open (appearance of pore clusters) porosity transition.

The function  $\chi$  must be formulated to describe the critical behaviour of the thermal conductivity of sintered metals from spherical particles. Many representations of critical functions are present in the literature.<sup>17,18</sup> Our goal is to propose a reliable physical model with few physical parameters, in order to be applicable on a wide range of metals. In this work we have considered the one proposed by Inden,<sup>19,20</sup> the ferromagnetic transition:

$$\chi(P) = A_{\pm} \ln \left[ \frac{1 + (P/P_c)^{\pm 3}}{1 + (P/P_c)^{\pm 3}} \right]. \quad (1)$$

In this equation, the symbol  $\pm$  means that the value is positive for  $P > P_c$  and negative otherwise. When  $P \rightarrow 1$ , the thermal conductivity is null. Consequently,  $A_{\pm}$  is constant in the entire range of porosity and it is trivial to show that

$$A_{\pm} = -\frac{\sqrt{3}}{\pi P_c}. \quad (2)$$

Thereafter, the integration of Eq. (1) gives

$$\lambda(P, d) = \lambda_0(d) \times \left( 1 + \int_0^P \chi(P') dP' \right). \quad (3)$$

In general  $\lambda_0$  also depends on the grain size. Indeed, when heat is conducted from one grain to another, the temperature is not continuous at the boundary, as there is a temperature jump,  $\Delta T$ . In the case where the heat flow,  $\Delta \dot{Q}$ , is small, one can assume a linear relationship between  $\Delta T$  and  $\Delta \dot{Q}$ . The thermal resistance across the grain boundary is defined as the ratio  $\frac{\Delta T}{\Delta \dot{Q}}$ . The degradation of the thermal conductivity, due to the thermal resistance across the grain boundaries, is often defined through the Kapitza formalism:<sup>5,6</sup>

$$\lambda_0(d) = \frac{\lambda_{\infty}}{1 + \frac{R_k \lambda_{\infty}}{d}}, \quad (4)$$

where  $R_k$ , the Kapitza resistance, is the average thermal resistance across the grain boundaries (assumed to be independent on the grain size distribution and orientation) and  $\lambda_{\infty}$  is the thermal

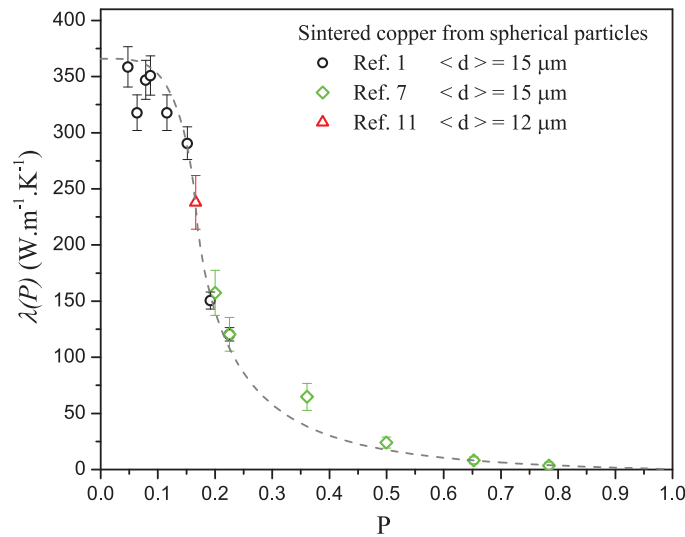


FIG. 3. Experimental thermal conductivity of sintered copper obtained from spherical particle (open symbols) in comparison with the model proposed in this work (dashed line). The unique adjustable parameter to describe the porosity dependence of the thermal conductivity is the critical porosity which is fixed to be 0.166.

conductivity of the dense monocrystal (i.e., non-porous with “infinite” grain size). It is worth pointing out that the Kapitza formalism was extended by Nan and Birringer<sup>21</sup> to take into account the grain size distribution. However, there are limitations: when the grain size distribution is not available (as with every experimental data in this work), we have to use Eq. (4).

In Fig. 3 we present the calculated  $\lambda(P)$  curve using Eq. (3) for sintered copper obtained from spherical particles. Assuming that  $\lambda_0(15 \mu\text{m}) = 366 \text{ W m}^{-1} \text{ K}^{-1}$  the Kapitza resistance is estimated to be  $3.5 \times 10^{-9} \text{ K m}^2 \text{ W}^{-1}$ . This value is in good agreement with the available experimental data close to room temperature reported by Gmelin *et al.*<sup>22</sup> which lies in the range  $1.85 \times 10^{-9} - 5.00 \times 10^{-9} \text{ K m}^2 \text{ W}^{-1}$ . The model prediction is in excellent agreement with the experimental data. Here, the Kapitza resistance is necessary only to calculate the thermal conductivity at zero porosity for a given average grain size of the considered microstructure. Therefore, only one adjustable model parameter is necessary to predict the porosity dependence of the thermal conductivity: the critical porosity.

In Fig. 4, considering the same  $P_c$  and  $R_k$  as for copper, we calculated the  $\lambda(P)$  curve of sintered silver from spherical particles. The model is in reasonable agreement with the only available set of experimental data<sup>3</sup> although some deviation is observed at  $P = 0.4$ . It is difficult to discuss the accuracy of the model for this point since only one set of experimental data is available and no error bars are reported. However, the difference between the model and the experimental point at  $P = 0.4$  is in the same range as the experimental error for sintered copper (see Fig. 1). In Fig. 5 we show the case of AISI 316L stainless steel, where we compare the results of the present model to the experimental data reported by Lima *et al.*<sup>2</sup> The model results match well with the experimental data. The critical porosity,  $P_c = 0.11$ , is lower than those of copper and silver. In a bond percolation problem, for a given function  $f$  of a variable  $x$ , the critical value  $x_c$  for which  $f(x)$  percolate is dependant on the coordination number. For systems in 8-fold and 12-fold coordination, the bond percolation is, respectively, 0.18 and 0.12.<sup>16</sup> These values are close to that we obtained for copper, silver, and stainless steel. The grain coordination number of sintered copper from spherical particle is estimated to be 7.2.<sup>23</sup> We have no information on the coordination number of the microstructure of silver and AISI 316L stainless. The percolation theory describes the simplest possible phase transition with nontrivial critical behaviour. The critical porosity of  $\lambda(P)$  of sintered metals from spherical particle powder may be close to that predicted by percolation theory; in this case, the present model can be fully predictive if enough information on the microstructure is available to quantify the average coordination number.

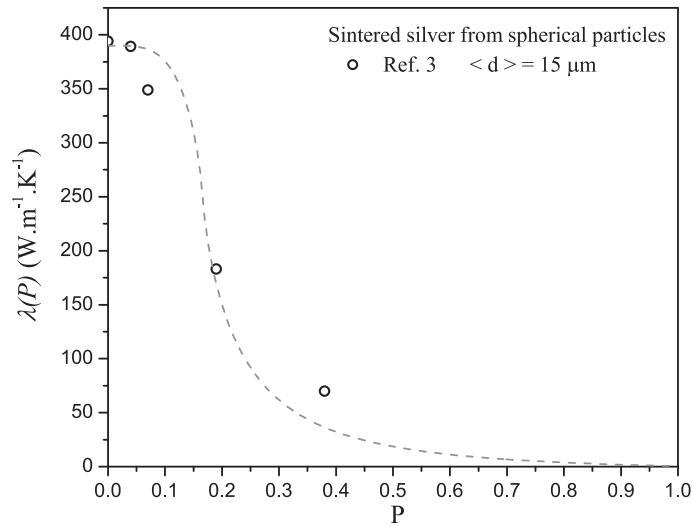


FIG. 4. Experimental thermal conductivity of sintered silver obtained from spherical particles (open symbols) in comparison with the model proposed in this work (dashed line). The unique adjustable parameter to describe the porosity dependence of the thermal conductivity is the critical porosity which is fixed to be identical to that of copper.

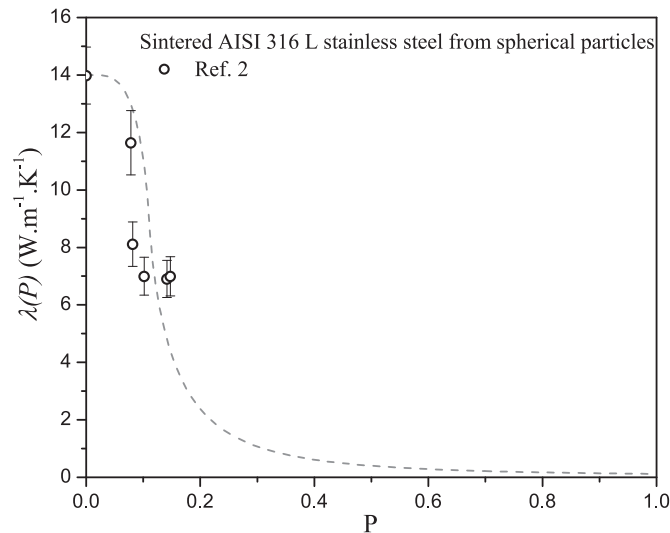


FIG. 5. Experimental thermal conductivity of sintered AISI 316L stainless steel obtained from spherical particles (open symbols) in comparison with the model proposed in this work (dashed line). The unique adjustable parameter to describe the porosity dependence of the thermal conductivity is the critical porosity which is fixed to be 0.11.

Due to a lack of data, the model presented in this paper is tested only for microstructures with microscale grains. A validation of the model for microstructures with nanoscale grains would make the model more robust. For the moment, the model is thus assumed valid only for microstructures with microscale grains.

In conclusion, we show that a second order phase transition induced by porosity is observed in sintered metal which is made from spherical particle powder with microscale grains. A simple model with a single adjustable parameter, the critical porosity, was proposed. The critical porosity may be linked to the average grain coordination number and has a value close to what is predicted by percolation theory. Experiments will be performed on other materials to confirm or disconfirm this assumption.

This research was supported by funding from the Natural Sciences and Engineering Research Council of Canada (NSERC) and Rio-Tinto-Alcan. This work was also partly funded by Carnot STAR Institute in the framework of a researcher exchange program. We thank Eve Bélisle and Dr. Jean-Philippe Harvey for stimulating discussions.

- <sup>1</sup> C. Vincent, J. Silvain, J. Heintz, and N. Chandra, *J. Phys. Chem. Solids* **73**, 499 (2012).
- <sup>2</sup> W. M. Lima, V. Biondo, W. R. Weinand, E. S. Nogueira, A. N. Medina, M. L. Baesso, and A. C. Bento, *J. Phys.: Condens. Matter* **17**, 1239 (2005).
- <sup>3</sup> A. A. Wereszczak, D. J. Vuono, H. Wang, and M. K. Ferber, Properties of bulk sintered silver as a function of porosity, ORNL/TM-2012/130, 2012.
- <sup>4</sup> J. Gibkes, B. Bein, D. Krger, and J. Pelzl, *Carbon* **31**, 801 (1993).
- <sup>5</sup> P. L. Kapitza, *J. Phys. USSR* **4**, 181 (1941).
- <sup>6</sup> H.-S. Yang, G.-R. Bai, L. Thompson, and J. Eastman, *Acta Mater.* **50**, 2309 (2002).
- <sup>7</sup> W. Mantle and W. S. Chang, in *Proceedings of the 24th Intersociety Energy Conversion Engineering Conference, 1989 (IECEC-89)* (IEEE, 1989), Vol. 4, pp. 1871–1877.
- <sup>8</sup> D. J. Thewsey and Y. Y. Zhao, *Phys. Status Solidi A* **205**, 1126 (2008).
- <sup>9</sup> EGG Ecka Granules GmbH, 2014, <http://www.ecka-granules.com/en/home/>.
- <sup>10</sup> EGG Ecka Granules GmbH, Copper and copper alloys, 2014, <http://www.ecka-granules.com/en/products/copper-and-copper-alloys/>.
- <sup>11</sup> See supplementary material at <http://dx.doi.org/10.1063/1.4886221> for a description of the experiment we have conducted to measure the thermal diffusivity of a sintered copper sample from spherical particles with a porosity level of 16.6%.
- <sup>12</sup> J. Kováčik, *Acta Mater.* **46**, 5413 (1998).
- <sup>13</sup> T. Velinov, K. Bransalov, and M. Mihovski, *Meas. Sci. Technol.* **4**, 1266 (1993).
- <sup>14</sup> J. Shackelford and W. Alexander, *CRC Materials Science and Engineering Handbook*, 3rd ed. (Taylor & Francis, 2010).
- <sup>15</sup> J. Kováčik and F. Šimančík, *Scr. Mater.* **39**, 239 (1998).
- <sup>16</sup> D. Stauffer and A. Aharony, *Introduction to Percolation Theory* (Taylor & Francis, 1992).
- <sup>17</sup> F. Gronvold, *Pure Appl. Chem.* **47**, 251 (1976).
- <sup>18</sup> R. Wielinga, in *Critical Behaviour in Magnetic Crystals*, Progress in Low Temperature Physics Vol. 6, edited by C. Gorter (Elsevier, 1970), Chap. 8, pp. 333–373.
- <sup>19</sup> G. Inden, in *Proceedings of CALPHAD V* (Max Planck Institut fuer Eisenforschung, 1976), pp. 1–13.
- <sup>20</sup> N. Saunders and A. Miodownik, *CALPHAD (CALculation of PHase Diagrams): A Comprehensive Guide*, Pergamon Materials Series Vol. 1, edited by R. W. Cahn (Elsevier Science, 1998).
- <sup>21</sup> C.-W. Nan and R. Birringer, *Phys. Rev. B* **57**, 8264 (1998).
- <sup>22</sup> E. Gmelin, M. Asen-Palmer, M. Reuther, and R. Villar, *J Phys D: Appl Phys.* **32**, R19 (1999).
- <sup>23</sup> C. Lautensack, K. Schladitz, and A. Sarka, in *Proceedings of 6th International Conference on Stereology, Spatial Statistics and Stochastic Geometrie*, 2006.